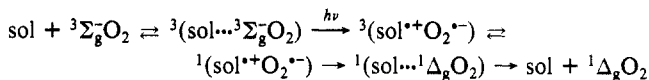


presence of a  $^1\Delta_g\text{O}_2$  quencher which also originates from the oxygen-solvent CT state.

We conclude, therefore, that  $^1\Delta_g\text{O}_2$  can be formed, in an appreciable yield, by a spin-allowed, oxygen ( $^3\Sigma_g^-\text{O}_2$ )-solvent cooperative transition to a triplet charge-transfer state with subsequent intersystem crossing and dissociation:



Our results can be regarded as experimental corroboration for the theoretical expectation of substantial mixing interactions between the CT state and other states of the oxygen-organic molecule complex [e.g.,  $^3(\text{M}^+\text{O}_2^{\cdot-}) \leftarrow (\text{mix}) \rightarrow ^3(^3\text{M}_1\cdots^3\Sigma_g^-\text{O}_2)$ ]. Thus, irradiation into the oxygen-organic molecule CT band provides an independent entry point to excited-state potential surfaces which, in turn, can be exploited to provide unique insight into the nature of oxygen-organic molecule interactions. For example, since  $^1\Delta_g\text{O}_2$  is also known to be formed in the process

of  $^3\Sigma_g^-\text{O}_2$ -induced  $^3\text{M}_1$  deactivation, a detailed study of  $^1\Delta_g\text{O}_2$  quantum yields, obtained from both a photosensitized experiment and CT excitation, can be helpful in evaluating matrix elements for state mixing. Finally, our results are expected to be important to scientists interested in methods by which organic materials and polymers photooxidize and degrade. In particular, we have shown that an excited state of molecular oxygen is easily formed, in the absence of sensitizers, in solvents thought to be inert.

**Acknowledgment.** This work was supported by the National Science Foundation under Grant CHE-8501542. The authors thank Professor M. R. Ondrias (UNM) for the use of his high-pressure Raman cell.

**Registry No.**  $\text{O}_2$ , 17778-80-2; mesitylene- $\text{O}_2$ , 76905-22-1; *p*-xylene- $\text{O}_2$ , 111130-05-3; *o*-xylene- $\text{O}_2$ , 111130-04-2; toluene- $\text{O}_2$ , 112270-21-0; benzene- $\text{O}_2$ , 50412-08-3; tetrahydrofuran- $\text{O}_2$ , 56596-57-7; 1,4-dioxane- $\text{O}_2$ , 120789-13-1; glyme- $\text{O}_2$ , 120789-14-2; diglyme- $\text{O}_2$ , 120789-15-3; triglyme- $\text{O}_2$ , 120789-16-4; methanol- $\text{O}_2$ , 120789-17-5; propanol- $\text{O}_2$ , 120789-18-6; cyclohexane- $\text{O}_2$ , 120789-19-7; cyclooctane- $\text{O}_2$ , 120789-20-0; decahydronaphthalene- $\text{O}_2$ , 120789-21-1.

## Thermal Decomposition of Alkyl Peroxynitrates

F. Zabel,\* A. Reimer, K. H. Becker, and E. H. Fink

*Physikalische Chemie, Fachbereich 9, Bergische Universität Gesamthochschule Wuppertal, Gausstrasse 20, 5600 Wuppertal 1, FRG (Received: December 6, 1988; In Final Form: February 22, 1989)*

The thermal decomposition of methyl peroxyxynitrate and ethyl peroxyxynitrate was studied in a temperature-controlled 420 L glass chamber at temperatures between  $-28$  and  $0^\circ\text{C}$  and total pressures from 10 to 800 mbar ( $M = \text{N}_2$ ). The reactions proceed via OO-N bond fission. The unimolecular decay of the peroxyxynitrates was followed in situ by long-path IR absorption using a Fourier transform spectrometer. In Troe's notation, the data are represented by the following limiting low- and high-pressure first-order rate constants  $k_0$  and  $k_\infty$  and the falloff curvature parameters  $F_c$ : for  $R = \text{CH}_3$ ,  $k_0/[\text{N}_2] = 9.0 \times 10^{-5} \exp(-80.6 \text{ kJ mol}^{-1}/RT) \text{ cm}^3 \text{ molecule}^{-1} \text{ s}^{-1}$ ,  $k_\infty = 1.1 \times 10^{16} \exp(-87.8 \text{ kJ mol}^{-1}/RT) \text{ s}^{-1}$ ,  $F_c = 0.4$ ; for  $R = \text{C}_2\text{H}_5$ ,  $k_0/[\text{N}_2] = 4.8 \times 10^{-4} \exp(-77.2 \text{ kJ mol}^{-1}/RT) \text{ cm}^3 \text{ molecule}^{-1} \text{ s}^{-1}$ ,  $k_\infty = 8.8 \times 10^{15} \exp(-86.8 \text{ kJ mol}^{-1}/RT) \text{ s}^{-1}$ ,  $F_c = 0.3$ . Combining the present results for  $R = \text{CH}_3$  with literature data on the corresponding recombination reaction,  $K_c = 1.94 \times 10^{27} \exp(-10766 \text{ K}/T) \text{ molecule cm}^{-3}$  is obtained for the equilibrium  $\text{CH}_3\text{OONO}_2 \rightleftharpoons \text{CH}_3\text{OO} + \text{NO}_2$ . Some experiments were performed on the thermal decomposition of isomeric mixtures of butyl, hexyl, and octyl peroxyxynitrate at 253 K and in 800 mbar of  $\text{N}_2$ . Atmospheric implications of the thermal stability of alkyl peroxyxynitrates are briefly discussed.

### Introduction

Peroxyxynitric acid ( $\text{HOONO}_2$ ) and organic peroxyxynitrates ( $\text{ROONO}_2$ ) represent potentially large atmospheric reservoirs for both peroxy radicals and reactive nitric oxides ( $\text{NO}_x = \text{NO} + \text{NO}_2$ ). The important role of  $\text{HOONO}_2$  for stratospheric chemistry has been recognized within the past decade, as a result of both model calculations<sup>1</sup> and field measurements.<sup>2</sup> Acetyl peroxyxynitrate (PAN) has been known as a main constituent of photochemical smog in urban environments for about 30 years.<sup>3</sup> Only recently it has been found to be ubiquitous in the troposphere with mixing ratios in the 10–1000 ppt range.<sup>4</sup> Similarly, the thermally less stable methyl peroxyxynitrate and, to a lesser extent, the higher alkyl peroxyxynitrates might be present in significant concentrations in the cooler regions of the atmosphere. So far, alkyl peroxyxynitrates have not been detected in the atmosphere,

but steady-state estimates suggest that a major part of  $\text{NO}_x$  may be tied up in  $\text{CH}_3\text{OONO}_2$  in the lower stratosphere.<sup>5</sup> For a more reliable assessment of the role which  $\text{CH}_3\text{OONO}_2$  and other alkyl peroxyxynitrates play in the troposphere and the stratosphere, the rate parameters for its most important source and loss processes must be known for the whole range of temperatures and pressures which are of atmospheric interest.

In the atmosphere,  $\text{CH}_3\text{OONO}_2$  is formed by the recombination of  $\text{CH}_3\text{OO}$  radicals with  $\text{NO}_2$ . Extensive laboratory measurements on this reaction have been performed at room temperature as a function of pressure for various collision partners<sup>6</sup> and as a function of pressure and temperature between 253 and 353 K.<sup>7</sup> The thermal decomposition of  $\text{CH}_3\text{OONO}_2$ , which is believed to reform  $\text{CH}_3\text{OO}$  and  $\text{NO}_2$ , was measured at a total pressure of 467 mbar between 256 and 268 K and at 253.1 K between 67 and 960 mbar, in both cases mostly with methane as a buffer gas.<sup>5</sup> From the combined results on recombination and dissociation rates, equilibrium constants and the heat of reaction for the thermal decomposition of  $\text{CH}_3\text{OONO}_2$  have been estimated.<sup>5</sup> The UV absorption cross sections of  $\text{CH}_3\text{OONO}_2$  were determined for  $200 \text{ nm} \leq \lambda \leq 310 \text{ nm}$ ,<sup>6,8-10</sup> with fairly large error limits in the im-

(1) (a) Jesson, J. P.; Glasgow, L. C.; Filkin, D. L.; Miller, C. *Geophys. Res. Lett.* **1977**, *4*, 513. (b) Sze, N. D.; Ko, M. K. W. *Atmos. Environ.* **1981**, *15*, 1301.

(2) Rinsland, C. P.; Zander, R.; Farmer, C. B.; Norton, R. H.; Brown, L. R.; Russell III, J. M.; Park, J. H. *Geophys. Res. Lett.* **1986**, *13*, 761.

(3) Stephens, E. R.; Hanst, P. L.; Doerr, R. C.; Scott, W. E. *Ind. Eng. Chem.* **1956**, *48*, 1498.

(4) (a) Singh, H. B.; Salas, L. J. *Nature* **1983**, *302*, 326. (b) Spicer, C. W.; Holdren, M. W.; Keigley, G. W. *Atmos. Environ.* **1983**, *17*, 1055. (c) Meyrahn, H.; Hahn, J.; Helas, G.; Warneck, P.; Penkett, S. A. *Proceedings of the 3rd European Conference Physico-Chemical Behaviour of Atmospheric Pollutants, 10-12 April 1984, Varese (Italy)*; Versino, B., Angeletti, G., Eds.; Reidel: Dordrecht, 1984; p 38.

(5) Bahta, A.; Simonaitis, R.; Heicklen, J. *J. Phys. Chem.* **1982**, *86*, 1849.

(6) Sander, S. P.; Watson, R. T. *J. Phys. Chem.* **1980**, *84*, 1664.

(7) Ravishankara, A. R.; Eisele, F. L.; Wine, P. H. *J. Chem. Phys.* **1980**, *73*, 3743.

(8) Cox, R. A.; Tyndall, G. S. *Chem. Phys. Lett.* **1979**, *65*, 357.

portant wavelength range  $\lambda \geq 270$  nm. From these data, it may be estimated that the photolysis rate of  $\text{CH}_3\text{OONO}_2$  under atmospheric conditions is of the same order as that of  $\text{HOONO}_2$  ( $J(\text{HOONO}_2) \sim 10^{-5} \text{ s}^{-1}$  for the troposphere<sup>11</sup>). The rate constant for the attack by OH radicals has not yet been determined but is expected to be similar to the rate constant for the reaction  $\text{CH}_3\text{C}(\text{O})\text{ONO}_2 + \text{OH} \rightarrow \text{products}$ , which was measured to be  $1.3 \times 10^{-13} \text{ cm}^3 \text{ molecule}^{-1} \text{ s}^{-1}$  at 298 K.<sup>12</sup> From these data it can be estimated that the lifetime of  $\text{CH}_3\text{OONO}_2$  in the upper troposphere and the lower stratosphere is probably controlled mainly by photolysis and thermal decomposition and that  $\text{CH}_3\text{OONO}_2$  may represent an important reservoir for both  $\text{NO}_x$  and  $\text{CH}_3\text{OO}$  radicals in certain regimes of the atmosphere, as was stated earlier.<sup>5</sup>

Similar to  $\text{CH}_3\text{OONO}_2$ , higher alkyl peroxy nitrates  $\text{ROONO}_2$  ( $\text{R} = \text{C}_2\text{H}_5, \text{C}_3\text{H}_7, \dots$ ) can be formed in the atmosphere by recombination of the corresponding ROO radicals with  $\text{NO}_2$ . A pressure-independent rate constant for the recombination of  $\text{C}_2\text{H}_5\text{OO}$  with  $\text{NO}_2$  was reported by Adachi and Basco.<sup>13</sup> No other data on the kinetic and photolytic properties of these peroxy nitrates are available except some results on the thermal stability of an isomeric mixture of *n*-propyl and isopropyl peroxy nitrate.<sup>14</sup>

Due to the limited range of experimental conditions and the use of methane as a buffer gas, extrapolations of the results of Bahta et al.<sup>5</sup> on the decomposition rate constants of  $\text{CH}_3\text{OONO}_2$  to the temperatures and pressures of the upper troposphere and the lower stratosphere remain uncertain. No data are available on the thermal stability of ethyl peroxy nitrate. For these reasons, the thermal decomposition of  $\text{CH}_3\text{OONO}_2$  and  $\text{C}_2\text{H}_5\text{OONO}_2$  has been studied in a temperature-controlled reaction chamber between  $-28$  and  $0^\circ\text{C}$  and over a wide pressure range, i.e., from 10 to 800 mbar, using  $\text{N}_2$  as a buffer gas. In addition, some experiments have been performed on the thermal decomposition of isomeric mixtures of butyl, hexyl, and octyl peroxy nitrate at 253 K and a total pressure of 800 mbar.

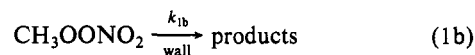
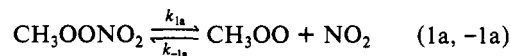
### Experimental Section

The temperature-controlled reaction chamber ( $-30$  to  $+50^\circ\text{C}$ ) has been described previously.<sup>15</sup> Briefly, it consists of a Duran glass tube (60-cm diameter, 420-L volume) with Teflon-coated aluminum end flanges. The reaction chamber is surrounded by 20 fluorescent lamps for photolysis at wavelengths above 300 nm. The temperature is continuously monitored in the gas phase, the ethanol coolant, and the end flanges.

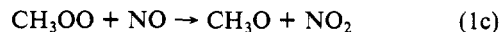
Temperatures were measured with an accuracy of  $\pm 0.2^\circ\text{C}$  and the temperature variation during a single experiment was  $< 0.1^\circ\text{C}$  at  $0^\circ\text{C}$  and  $< 0.8^\circ\text{C}$  at  $-20^\circ\text{C}$ . The concentrations of  $\text{CH}_3\text{OONO}_2$  and other compounds were monitored by in situ infrared absorption spectroscopy using a multireflection White mirror system (base length 1.4 m, optical path length 50.4 m) which was coupled to an FTIR spectrometer (Nicolet 7199, Globar light source, HgCdTe detector). Infrared absorption spectra were recorded at  $1\text{-cm}^{-1}$  spectral resolution by coadding 2–60 interferograms over periods from 4 to 120 s. Total reaction times were between 1 and 30 min.

Before starting an experiment, the reaction chamber was evacuated to pressures below 0.002 mbar. In a typical experiment on the thermal decomposition of  $\text{CH}_3\text{OONO}_2$ , nitrogen was added to a mixture of 0.1 mbar of azomethane, 0.01 mbar of  $\text{NO}_2$ , and

2.4 mbar of  $\text{O}_2$  up to the desired total pressure. Photolysis of this gas for 60 min resulted in a mixture of  $\sim 0.003$  mbar of  $\text{CH}_3\text{OONO}_2$ ,  $\sim 0.002$  mbar of  $\text{NO}_2$ , and  $\sim 0.010$  mbar of  $\text{H}_2\text{CO}$ . The wall loss of  $\text{CH}_3\text{OONO}_2$  was measured in the dark for about 15 min. During that time, equilibrium was maintained between  $\text{CH}_3\text{OONO}_2$  and its decomposition products  $\text{CH}_3\text{OO}$  and  $\text{NO}_2$ , with a small fraction of  $\text{CH}_3\text{OONO}_2$  disappearing on the walls:



Finally, the decay of  $\text{CH}_3\text{OONO}_2$  due to thermal decomposition in the gas phase was initiated by the addition of  $\sim 0.3$  mbar of NO. Then the following additional reactions occur:



By applying sufficiently large amounts of NO, reaction -1a cannot compete with reaction 1c and the first-order decay rate of the concentration of  $\text{CH}_3\text{OONO}_2$  is solely determined by the rate of reaction 1a.

The higher alkyl peroxy nitrates ( $\text{ROONO}_2$ ) were produced in situ by photolyzing highly diluted mixtures of RH,  $\text{Cl}_2$ ,  $\text{O}_2$ , and  $\text{NO}_2$  in  $\text{N}_2$  for 5–10 min. Typical initial partial pressures of  $\text{ROONO}_2$  were 0.003–0.006 mbar. The subsequent analysis was as outlined above for  $\text{CH}_3\text{OONO}_2$ .

The decay of  $\text{CH}_3\text{OONO}_2$  and  $\text{ROONO}_2$  before and after the addition of NO was monitored as a function of time. The IR absorption bands of  $\text{CH}_3\text{OONO}_2$  and  $\text{ROONO}_2$  were identified by their fast decay in the presence of NO and by comparison with the corresponding  $\text{ROONO}_2$  spectra from Niki et al.<sup>16</sup> Relative  $\text{CH}_3\text{OONO}_2$  concentrations were determined by using the IR absorption band centered at  $1724 \text{ cm}^{-1}$  after computer subtraction of overlapping absorptions from  $\text{H}_2\text{CO}$ ,  $\text{HCOOH}$ , and  $\text{HONO}$ . Under certain reaction conditions there was some interference from  $\text{HOCH}_2\text{OONO}_2$ , which is formed from  $\text{H}_2\text{CO}$  and  $\text{HO}_2$  in the presence of  $\text{NO}_2$  and decomposes with a rate comparable to that of  $\text{CH}_3\text{OONO}_2$ .<sup>17</sup> In such cases, the  $1725\text{-cm}^{-1}$  absorption band of  $\text{HOCH}_2\text{OONO}_2$  was also subtracted. The relative concentrations of  $\text{C}_2\text{H}_5\text{OONO}_2$ ,  $\text{C}_4\text{H}_9\text{OONO}_2$ ,  $\text{C}_6\text{H}_{13}\text{OONO}_2$ , and  $\text{C}_8\text{H}_{17}\text{OONO}_2$  were monitored using their strongest IR absorption bands at 1719, 1718, 1715, and  $1715 \text{ cm}^{-1}$ , respectively. It was regularly checked that no residual absorption remained at these wavelengths after long reaction times. No subtraction of overlapping absorption features was necessary in these cases, resulting in more precise data. In particular, the scatter in the  $\text{C}_2\text{H}_5\text{OONO}_2$  data was considerably less as compared to the  $\text{CH}_3\text{OONO}_2$  data. Several isomers were formed during the preparation of  $\text{C}_4\text{H}_9\text{OONO}_2$ ,  $\text{C}_6\text{H}_{13}\text{OONO}_2$ , and  $\text{C}_8\text{H}_{17}\text{OONO}_2$ . As the IR bands of the different isomers could not be resolved, the thermal decay rates of isomeric mixtures have been determined for these peroxy nitrates. Initial and final NO and  $\text{NO}_2$  concentrations were also regularly measured. No attempts were made in the present experiments to determine carbon and nitrogen mass balances.

Azomethane was prepared from *N,N'*-dimethylhydrazinium dichloride and  $\text{CuCl}_2$  according to the method of Jahn.<sup>18</sup> Research grade ethane, *n*-butane, *n*-hexane, *n*-octane, NO,  $\text{NO}_2$ ,  $\text{N}_2$ , and  $\text{O}_2$  were used.  $\text{NO}_2$  impurities in NO were removed by fractionated distillation from a liquid nitrogen trap.

### Results and Discussion

The logarithmic plots of  $\text{ROONO}_2$  concentrations as a function of time were found to be linear before and after NO addition, with a marked increase of the slope at the point of NO addition. The

(9) Morel, O.; Simonaitis, R.; Hecklen, J. *Chem. Phys. Lett.* **1980**, *73*, 38.  
 (10) Baulch, D. L.; Cox, R. A.; Crutzen, P. J.; Hampson, R. F., Jr.; Kerr, J. A.; Troe, J.; Watson, R. T. *J. Phys. Chem. Ref. Data* **1982**, *11*, 327.  
 (11) Molina, L. T.; Molina, M. J. *J. Photochem.* **1981**, *15*, 97.  
 (12) Wallington, T. J.; Atkinson, R.; Winer, A. M. *Geophys. Res. Lett.* **1984**, *11*, 861.  
 (13) Adachi, H.; Basco, N. *Chem. Phys. Lett.* **1979**, *67*, 324.  
 (14) Edney, E. O.; Spence, J. W.; Hanst, P. L. *J. Air Pollut. Control Assoc.* **1979**, *29*, 741.  
 (15) (a) Barnes, I.; Becker, K. H.; Fink, E. H.; Reimer, A.; Zabel, F.; Niki, H. *Int. J. Chem. Kinet.* **1983**, *15*, 631. (b) Barnes, I.; Bastian, V.; Becker, K. H.; Fink, E. H.; Kriesche, V.; Nelsen, W.; Reimer, A.; Zabel, F. In "Untersuchung der Reaktionssysteme  $\text{NO}_x/\text{ClO}_x/\text{HO}_x$  unter troposphärischen Bedingungen"; *BPT-Ber.* **1984**, *11/84*.

(16) Niki, H.; Maker, P. D.; Savage, C. M.; Breitenbach, L. P. *Chem. Phys. Lett.* **1978**, *55*, 289.

(17) Barnes, I.; Becker, K. H.; Fink, E. H.; Reimer, A.; Zabel, F.; Niki, H. *Chem. Phys. Lett.* **1985**, *115*, 1.

(18) Jahn, F. P. *J. Am. Chem. Soc.* **1937**, *59*, 1761.

ROONO<sub>2</sub> decay before addition of NO was attributed to wall loss. The rate constant  $k_b$  varied from experiment to experiment but was constant for a single experiment. This behavior is well-known from other thermally unstable compounds (e.g., HOONO<sub>2</sub><sup>19</sup>). The ROONO<sub>2</sub> decay after NO addition was attributed to reactions a and b. The gas-phase decomposition rate constant  $k_a$  was then obtained from the difference of both slopes before and after NO addition.

In the experimental pressure range,  $k_a$  proved to be strongly pressure dependent for CH<sub>3</sub>OONO<sub>2</sub> and slightly pressure dependent for C<sub>2</sub>H<sub>5</sub>OONO<sub>2</sub>. The pressure dependence of  $k_a$  was evaluated by using the three-parameter representation of RRK(M) falloff curves as suggested by Troe and co-workers.<sup>20-22</sup> The simplest version recommended by Luther and Troe<sup>20</sup> was adopted:

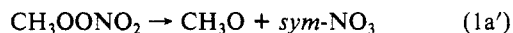
$$\log \frac{k}{k_\infty} = \log \frac{k_0/k_\infty}{1 + k_0/k_\infty} + \frac{\log F_c}{1 + \left[ \frac{\log(k_0/k_\infty)}{N(F_c)} \right]^2} \quad (\text{I})$$

where

$$N(F_c) = 0.75 - 1.27 \log F_c \quad (\text{ref 21})$$

In eq I,  $k_0$  and  $k_\infty$  are the low- and high-pressure limiting first-order rate constants, respectively, and  $F_c$  is a curvature parameter closely related to the vibrational structure of the decomposing molecule.

**Methyl Peroxynitrate.** In addition to 1a, two other unimolecular decomposition steps are conceivable for the thermal decomposition of CH<sub>3</sub>OONO<sub>2</sub>:



As both (1a) and (1a') are simple bond fission reactions, similar preexponential factors are expected for  $k_{1a}$  and  $k_{1a'}$  such that the decomposition rates at low temperatures are largely determined by the bond energy. With the use of data from the most recent CODATA evaluation<sup>23</sup> and from Benson,<sup>24</sup>  $\Delta H_f^\circ$  is estimated to be larger for (1a') by  $\sim 25$  kJ mol<sup>-1</sup>, corresponding to a rate slower by a factor of  $\sim 10^5$  at 260 K and thus strongly favoring channel 1a. Reaction 1a'' is exothermic by  $\sim 35$  kJ mol<sup>-1</sup> and could proceed via a five-center transition state. Very recently, a corresponding reaction channel has been proposed for the thermal decomposition of acetyl peroxyxynitrate (PAN) as a minor decomposition pathway, with CH<sub>3</sub>ONO<sub>2</sub> and CO<sub>2</sub> as the observed products.<sup>25</sup> As thermochemistry is less favorable for such a concerted mechanism in the case of CH<sub>3</sub>OONO<sub>2</sub>, (1a'') is considered to be unimportant. In particular, the strong dependence of the CH<sub>3</sub>OONO<sub>2</sub> decay rate on the presence of NO is in favor of reaction 1a.

The first-order decomposition rate of CH<sub>3</sub>OONO<sub>2</sub> could be measured for thermal lifetimes between 30 and 3800 s.  $k_{1a}$  proved to be strongly pressure dependent, in agreement with previous measurements on reactions 1a<sup>5</sup> and -1a.<sup>6,7</sup> For this reason, the thermal decomposition was measured at total pressures of 10, 30, 100, 300 and 800 mbar for M = mainly N<sub>2</sub>. All of these reaction mixtures contained a constant oxygen partial pressure of 2.4 mbar which was necessary for the in situ generation of CH<sub>3</sub>OONO<sub>2</sub> from CH<sub>3</sub>N<sub>2</sub>CH<sub>3</sub>. The pressure dependence of  $k_{1a}$  was measured

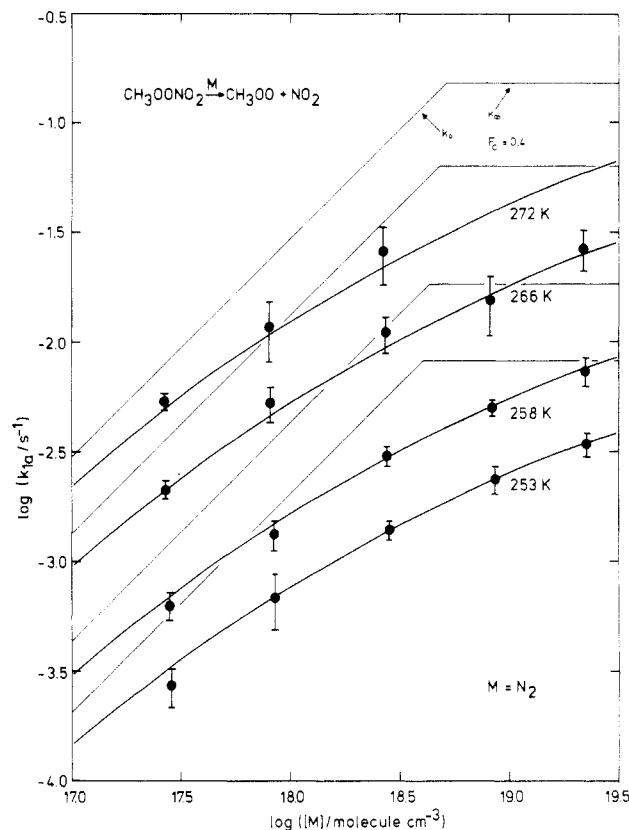


**Figure 1.** Pressure dependence of  $k_{1a}$  at different temperatures for M = N<sub>2</sub>. ●, average of at least four individual rate constants with 2 $\sigma$  errors; straight lines,  $k_0 = k_{2\text{nd order}}[\text{N}_2]$  and  $k_\infty$ ; curves, falloff curves according to eq I (see text).

at four different temperatures: -20, -15, -7.5, and 0 °C. At each temperature/pressure combination at least four individual measurements were performed. The results are summarized in Table I and illustrated in Figure 1.

The effective first-order gas-phase decay rate constants for CH<sub>3</sub>OONO<sub>2</sub>,  $k_{1a,\text{eff}}$ , correspond to  $k_{1a}$  only in case where the [NO]/[NO<sub>2</sub>] ratio is large enough such that reaction -1a cannot compete with reaction 1c. This was achieved experimentally by using large initial NO partial pressures. Typically, the [NO]/[NO<sub>2</sub>] ratio changed from  $\sim 100$  to  $\sim 20$  in the course of an experiment. As both  $k_{-1a}$  as a function of temperature, pressure, and collision partner<sup>6,7</sup> and  $k_{1c}$ <sup>23</sup> are well-known, the deviation of the measured rate constant  $k_{1a,\text{eff}}$  from  $k_{1a}$  could be estimated from computer simulations of the experimental data.  $k_{1a,\text{eff}}$  was not corrected whenever the estimated ratio  $(k_{1a,\text{eff}} - k_{1a})/k_{1a,\text{eff}}$  was lower than 1%. In about 20% of the measurements, this ratio was smaller than 5% but higher than 1%. In these cases, the effective rate constants were corrected by using  $k_{-1a}$  from Ravishankara et al.<sup>7</sup> and Sander and Watson<sup>6</sup> and  $k_{1c}$  from Baulch et al.<sup>23</sup>

The rate constants in Table I were determined at temperatures slightly scattering around certain mean temperatures which were close to  $T_m = 253, 258, 266,$  and  $272$  K, respectively. The falloff of  $k_{1a}$  with decreasing pressure is shown in Figure 1. As  $k_{1a}$  is strongly temperature dependent, the rate constants of the fourth column in Table I have been adjusted to the corresponding temperatures  $T_m$  and averaged (last column of Table I), using an activation energy of 85 kJ mol<sup>-1</sup>, which is between the finally selected values for the activation energies of reaction 1a in the high- and low-pressure limits (see below). An error of 10 kJ mol<sup>-1</sup> for this activation energy would result in errors  $< 1\%$  for  $k_{1a}(T_m)$ . Thus, each experimental point in Figure 1 represents the average of at least four independently measured  $k_{1a}$  values which have been adjusted to the temperature  $T_m$  indicated at the corresponding falloff curve. The error bars correspond to 2 $\sigma$  errors.

The value  $F_c$  in eq I was obtained in two ways:

(19) Graham, R. A.; Winer, A. M.; Pitts, J. N., Jr. *J. Chem. Phys.* **1978**, *68*, 4505.

(20) Luther, K.; Troe, J. *17th Symposium (International) on Combustion*; The Combustion Institute: Pittsburgh, 1979; p 535.

(21) Troe, J. *J. Phys. Chem.* **1979**, *83*, 114.

(22) Gilbert, R. G.; Luther, K.; Troe, J. *Ber. Bunsen-Ges. Phys. Chem.* **1983**, *87*, 169.

(23) Baulch, D. L.; Cox, R. A.; Hampson, R. F., Jr.; Kerr, J. A.; Troe, J.; Watson, R. T. *J. Phys. Chem. Ref. Data* **1984**, *13*, 1259.

(24) Benson, S. W. *Thermochemical Kinetics*, 2nd ed.; Wiley: New York, 1976.

(25) Senum, G. I.; Fajer, R.; Gaffney, J. S. *J. Phys. Chem.* **1986**, *90*, 152.

TABLE I: Summary of First-Order Rate Constants for the Thermal Decomposition ( $k_{1a}$ ) and the Wall Loss ( $k_{1b}$ ) of  $\text{CH}_3\text{OONO}_2^a$ 

run no.	T, K	$p_{\text{tot}}$ , mbar	$k_{1a}$ , $10^{-4} \text{ s}^{-1}$	$k_{1b}$ , $10^{-4} \text{ s}^{-1}$	$k_{1a,av}$ , $10^{-4} \text{ s}^{-1} (T_m)$	run no.	T, K	$p_{\text{tot}}$ , mbar	$k_{1a}$ , $10^{-4} \text{ s}^{-1}$	$k_{1b}$ , $10^{-4} \text{ s}^{-1}$	$k_{1a,av}$ , $10^{-4} \text{ s}^{-1} (T_m)$
M = N <sub>2</sub>											
1	253.15	800	34.6	0.9		48	265.6	800	247	1	
2	253.15	800	32.6	1.2	34.3 ± 4.3 (253 K)	49	265.8	800	266	1	
3	253.15	801	35.2	1.5		50	265.8	800	302	1	267 ± 57 (266 K)
4	253.25	800	38.5	0.9		51	265.45	798	217	2	
5	253.2	300	26.4	1.3		52	265.5	800	236	2	
6	253.05	299	25.3	0.8	23.8 ± 3.5 (253 K)	53	265.65	300	126	3	
7	253.1	300	22.6	1.4		54	265.85	304	124	2	
8	253.2	300	23.1	0.6		55	265.7	300	120	3	
9	253.05	97	14.3	1.3		56	265.15	300	122	4	155 ± 48 (266 K)
10	253.1	100	13.1	2.3		57	265.65	300	189	1	
11	253.15	100	15.1	0.9	13.9 ± 1.4 (253 K)	58	265.8	300	152	3	
12	253.15	100	13.7	1.4		59	265.95	300	174	1	
13	253.15	100	14.5	1.0		60	265.65	300	150	3	
14	253.15	30.1	7.72	0.94		61	265.65	300	166	3	
15	253.15	30.0	6.55	1.15	6.84 ± 1.95 (253 K)	62	265.65	300	152	5	
16	253.25	30.1	8.06	0.54		63	265.35	101	105	2	
17	252.9	30.1	5.59	1.16		64	265.65	100	108	2	110 ± 21 (266 K)
18	253.15	10.1	2.72	1.08		65	265.95	100	93	3	
19	253.1	10.1	3.02	0.52	2.71 ± 0.54 (253 K)	66	265.3	100	106	2	
20	253.25	10.1	2.98	0.60		67	265.55	30.1	44.6	2.0	
21	253.1	10.1	2.40	0.95		68	265.45	30.0	48.4	1.4	52.7 ± 9.7 (266 K)
22	258.25	797	83.4	0.6		69	265.7	30.1	49.2	2.1	
23	258.0	800	73.4	0.5		70	265.3	30.1	53.5	2.0	
24	258.2	800	66.9	1.3	73.9 ± 11.3 (258 K)	71	264.95	10.1	17.9	2.4	
25	258.05	800	76.5	0.5		72	265.65	10.1	20.4	2.2	21.4 ± 2.0 (266 K)
26	258.15	800	76.7	1.9		73	265.55	10.0	19.2	2.5	
27	258.2	304	52.0	1.0		74	265.7	10.0	21.8	2.4	
28	258.3	300	53.2	0.9		75	272.3	100	249	5	
29	258.25	300	50.1	1.2	50.0 ± 4.3 (258 K)	76	272.25	100	245	4	258 ± 76 (272 K)
30	258.2	300	54.5	1.8		77	272.15	100	247	3	
31	258.15	301	48.7	1.6		78	271.95	100	313	5	
32	257.75	100	28.9	2.3		79	272.3	30.0	126	4	
33	257.75	100	27.7	1.5		80	272.05	30.0	141	4	117 ± 36 (272 K)
34	257.85	100	32.0	1.3	30.4 ± 3.2 (258 K)	81	272.35	30.0	103	3	
35	257.85	100	30.9	1.3		82	272.1	30.1	111	3	
36	258.2	100	29.4	1.2		83	272.3	10.1	56.5	2.5	
37	258.2	100	31.4	1.7		84	272.35	10.0	53.8	1.1	53.8 ± 4.3 (272 K)
38	258.1	30.0	12.2	1.1		85	272.2	10.1	54.8	2.8	
39	258.0	30.0	14.5	0.4	13.3 ± 2.1 (258 K)	86	272.0	10.0	56.5	3.0	
40	258.05	30.1	13.2	1.3		M = O <sub>2</sub>					
41	258.1	30.0	13.9	1.6		87	257.95	10.3	7.8	1.6	
42	258.05	10.0	5.62	0.92		88	257.45	10.0	5.9	0.7	
43	257.9	9.9	5.98	0.25		89	257.75	10.1	5.7	0.3	
44	257.65	10.1	6.60	2.12	6.31 ± 0.94 (258 K)	90	258.1	10.0	6.7	0.8	6.84 ± 1.36 (258 K)
45	258.15	10.1	6.40	1.61		91	258.15	10.0	7.2	1.2	
46	258.05	9.9	6.62	1.48		92	258.1	10.0	7.8	1.5	
47	258.15	10.0	6.58	1.04		93	258.05	10.1	6.9	2.1	
						94	258.05	10.1	6.4	0.7	

<sup>a</sup>Rate constants of the last column are *not* the average of those of the fourth column due to slightly different temperatures.

(i) Equation I was fitted to the experimental data points in Figure 1 for 266 and 258 K by use of a least-squares computer program and application of  $N(F_c) = 0.75 - 1.27 \log F_c$ .<sup>21,22</sup>  $F_c = 0.43 \pm 0.20$  ( $2\sigma$ ) and  $F_c = 0.54 \pm 0.30$  ( $2\sigma$ ) were obtained for 266 and 258 K, respectively. As  $F_c$  is estimated to increase only by  $\sim 0.01$  on going from 266 to 258 K, and considering the large error limits of the experimental  $F_c$  values as presented above, it was decided to neglect the temperature dependence of  $F_c$  for the present evaluation. Thus a weighted mean value of 0.47 was deduced for the temperature range from  $-20$  to  $0^\circ\text{C}$ .

(ii)  $F_c$  may be estimated from the vibrational frequencies of  $\text{CH}_3\text{OONO}_2$  by the methods described by Troe et al.<sup>20-22</sup> Most fundamentals were estimated with acetyl peroxynitrate as a model compound since for this molecule a fairly complete vibrational assignment exists in the literature.<sup>26</sup> The three torsional frequencies were adjusted to give the correct entropy at 300 K as estimated from group additivity rules.<sup>24,27</sup> The applied frequencies

are collected in Table II. With these figures and with  $E_0 = 86.2 \text{ kJ mol}^{-1}$  (see below),  $F_c = 0.35$  is obtained, allowing for weak collision effects (with an estimated  $\beta_c = k_0/k_0^{sc} = 0.2$  for  $M = \text{N}_2$ ).

Considering the uncertainties in the experimental and theoretical  $F_c$  values from (i) and (ii) above and the difference between both values,  $F_c = 0.4$  was adopted for the evaluation of the present rate data. This value is identical with  $F_c = 0.40 \pm 0.10$  as experimentally obtained by Sander and Watson<sup>6</sup> for the reverse reaction ( $-1a$ ) in a smaller pressure range but for three different collision partners ( $M = \text{He}, \text{N}_2, \text{SF}_6$ ).

For atmospheric applications, a simplified version of eq I with  $N(F_c) = 1$  has been suggested<sup>21,29</sup> and adopted.<sup>10,23,30</sup> Even though

(27) Patrick, R.; Golden, D. M. *Int. J. Chem. Kinet.* **1983**, *15*, 1189.

(28) Hohorst, F. A.; DesMarteau, D. D. *Inorg. Chem.* **1974**, *13*, 715.

(29) Zellner, R. *Ber. Bunsen-Ges. Phys. Chem.* **1978**, *82*, 1172.

(30) DeMore, W. B.; Molina, M. J.; Sander, S. P.; Golden, D. M.; Hampson, R. F.; Kurylo, M. J.; Howard, C. J.; Ravishankara, R. F. *JPL Publ.* **1987**, *87-41*.

(26) Bruckmann, P. W.; Willner, H. *Environ. Sci. Technol.* **1983**, *17*, 352.

TABLE II: Estimated Vibrational Frequencies for CH<sub>3</sub>OONO<sub>2</sub>

wavenumber cm <sup>-1</sup>		model compd	ref
3040	CH <sub>3</sub> asym stretch	PAN	26
3022	CH <sub>3</sub> asym stretch	PAN	26
2951	CH <sub>3</sub> sym stretch	PAN	26
1724 <sup>a</sup>	NO <sub>2</sub> asym stretch		16
1430	CH <sub>3</sub> asym deform	PAN	26
1430	CH <sub>3</sub> asym deform	PAN	26
1371	CH <sub>3</sub> sym deform	PAN	26
1299 <sup>a</sup>	NO <sub>2</sub> sym stretch		16
1055	CH <sub>3</sub> rock	PAN	26
1055	CH <sub>3</sub> rock	PAN	26
988 <sup>a</sup>	CO stretch <sup>b</sup>		16
880	OO stretch	CF <sub>3</sub> OONO <sub>2</sub>	28
821	NO stretch	PAN	26
791 <sup>a</sup>	NO <sub>2</sub> deform		16
716	NO <sub>2</sub> wag	PAN	26
488		PAN	26
370		PAN	26
338		PAN	26
120	torsion		27
45 <sup>c</sup>	torsion		27
45 <sup>c</sup>	torsion		27

<sup>a</sup> Measured (ref 16 and this work). <sup>b</sup> Assignment by comparison with CH<sub>3</sub>OONO<sub>2</sub> ( $\nu_{\text{CO}} = 1018 \text{ cm}^{-1}$ )<sup>16</sup> and CF<sub>3</sub>OONO<sub>2</sub> ( $\nu_{\text{CO}} = 953 \text{ cm}^{-1}$ )<sup>28</sup>. <sup>c</sup> Slightly adjusted to give the entropy of CH<sub>3</sub>OONO<sub>2</sub> as estimated in ref 27.

this approximation gives results that differ from those obtained with  $N(F_c) = 0.75 - 1.27 \log F_c$ <sup>21</sup> by at most 10% in the experimentally covered pressure range, distortions of the reduced falloff curve are introduced by this approximation which may lead to much larger errors for  $k_0$  and/or  $k_\infty$  for  $F_c < 0.5$ , in unfavorable cases. For this reason,  $N(F_c) = 0.75 - 1.27 \log F_c$  was applied throughout the present work. The  $k_0$  and  $k_\infty$  values thus derived for the temperatures 253, 258, 266, and 272 K were slightly adjusted in order to obtain simple Arrhenius expressions. According to this procedure, the following set of parameters was obtained which, when applied to eq I, describes all of the present experimental results for M = N<sub>2</sub> within  $\pm 10\%$ :

$$F_c = 0.4$$

$$k_0/[N_2] = 9.0 \times 10^{-5} \exp(-80.6 \text{ kJ mol}^{-1}/RT) \text{ cm}^3 \text{ molecule}^{-1} \text{ s}^{-1}$$

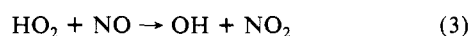
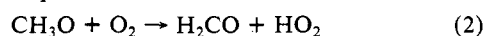
$$k_\infty = 1.1 \times 10^{16} \exp(-87.8 \text{ kJ mol}^{-1}/RT) \text{ s}^{-1}$$

At a total pressure of 10 mbar, a considerable proportion ( $\sim 25\%$ ) of the buffer gas was oxygen rather than nitrogen. Several experiments have been performed in pure oxygen at  $-7.5^\circ \text{C}$  and at low total pressures (10 mbar) in order to evaluate the influence of this oxygen content on the rate constant  $k_{1a}$  deduced for M = N<sub>2</sub>. Under these reaction conditions, (i) the error limits of  $k_{1a}$  are low and (ii) different collision efficiencies should have a large effect on  $k_{1a}$ . The results of these experiments are included in Table I. The average  $k_{1a}$  values obtained in 2.4 mbar of O<sub>2</sub> + 7.7 mbar of N<sub>2</sub> and in 10.1 mbar of O<sub>2</sub> are similar resulting in a  $k_0(\text{M}=\text{O}_2)/k_0(\text{M}=\text{N}_2)$  ratio of  $1.15 \pm 0.20$ . In deriving this value,  $F_c$  and  $k_\infty$  have been assumed to be the same for M = N<sub>2</sub> and M = O<sub>2</sub>. For dry air, an effective limiting low-pressure rate constant of

$$k_0(\text{dry air}) = 1.03k_0(\text{N}_2)$$

is obtained from these figures.

Evaluation of the rate constants in Table I is based on the assumption that the CH<sub>3</sub>OONO<sub>2</sub> decay proceeds only by reactions 1a and 1b. On the other hand, reactive OH radicals are formed via the reaction sequence:



Using rate constants from the CODATA evaluations,<sup>10,23</sup> it may be estimated that, under the present reaction conditions, OH is

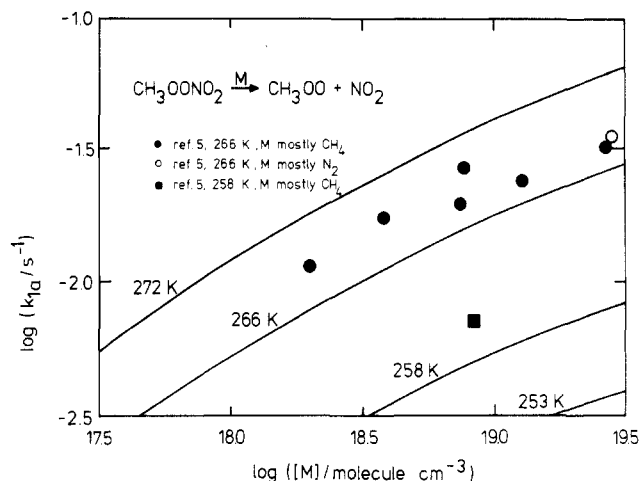
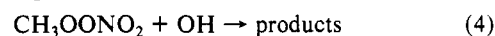
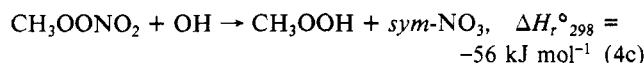
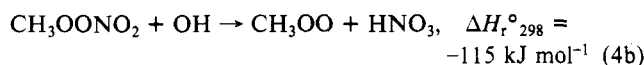
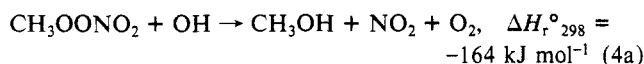


Figure 2. Comparison of present data on  $k_{1a}$  with literature. Full curves, present data, from Figure 1; ●, ref 5, M = CH<sub>4</sub>, converted to  $T = 266 \text{ K}$  from  $263.3 \text{ K}$  (ref 5) using eq I; ■, ref 5, M = CH<sub>4</sub>.

consumed nearly exclusively by reactions with NO, H<sub>2</sub>CO, NO<sub>2</sub>, HONO, and CO provided that the rate constant for the reaction with CH<sub>3</sub>OONO<sub>2</sub>, reaction 4,



is  $\leq 10^{-11} \text{ cm}^3 \text{ molecule}^{-1} \text{ s}^{-1}$ . Unfortunately, no experimental data are available on reaction 4. This reaction most likely proceeds by H atom abstraction. If this is true,  $k_4 \sim 10^{-13} \text{ cm}^3 \text{ molecule}^{-1} \text{ s}^{-1}$  at 298 K can be estimated by comparison with the corresponding rate data on OH + alkanes,<sup>31</sup> OH + CH<sub>3</sub>C(O)CH<sub>3</sub>,<sup>32</sup> and OH + CH<sub>3</sub>C(O)OONO<sub>2</sub>.<sup>12</sup> On the other hand,  $k_4 \sim 6 \times 10^{-12} \text{ cm}^3 \text{ molecule}^{-1} \text{ s}^{-1}$  results if reaction 4 is as fast as the attack on the methyl group in CH<sub>3</sub>OOH.<sup>33</sup> In either case, reaction 4 is unimportant under the conditions of the present experiments. Another possible pathway is the addition of OH with the following reaction channels:



( $\Delta H_f^\circ_{298}(\text{CH}_3\text{OONO}_2)$  from this work, see below; other enthalpies from DeMore et al.<sup>30</sup>). Addition reactions of this type possibly occur with OH + HNO<sub>3</sub><sup>34</sup> and OH + HOONO<sub>2</sub>,<sup>35</sup> where large rate constants ( $> 10^{-12} \text{ cm}^3 \text{ molecule}^{-1} \text{ s}^{-1}$ ) and slightly negative activation energies have been determined experimentally. If this were the case, reaction 4 could play a role at low temperatures both in laboratory experiments and in the atmosphere. The same arguments hold for the reaction of OH with acetyl peroxyxynitrate. For this reaction, a rate constant of  $\sim 1 \times 10^{-13} \text{ cm}^3 \text{ molecule}^{-1} \text{ s}^{-1}$  at 298 K and a positive activation energy have been determined by Wallington et al.<sup>12</sup> which is typical for an H atom abstraction. For this reason, we believe reaction 4 to be an H atom abstraction not interfering with the thermal decomposition reaction (1a).

The present results on  $k_{1a}$  may be compared with the work of Bahta et al.<sup>5</sup> These authors measured  $k_{1a}$  by monitoring the NO<sub>2</sub> formation via UV absorption. They used methane as a bath gas

(31) Atkinson, R.; Carter, W. P. L.; Aschmann, S. M.; Winer, A. M.; Pitts, J. N., Jr. *Int. J. Chem. Kinet.* **1984**, *16*, 469.

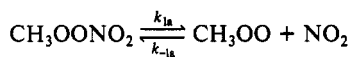
(32) Becker, K. H.; Biehl, H. M.; Bruckmann, P.; Fink, E. H.; Fuhr, F.; Klöpfer, W.; Zellner, R.; Zetzsch, C. In "Methods of the Ecotoxicological Evaluation of Chemicals. Photochemical Degradation in the Gas Phase, Vol. 6"; *Spez. Ber. Kernforschungsanlage Juelich* **1984**, *Juel-Spez-279*.

(33) Niki, H.; Maker, P. D.; Savage, C. M.; Breitenbach, L. P. *J. Phys. Chem.* **1983**, *87*, 2190.

(34) Margitan, J. J.; Watson, R. T. *J. Phys. Chem.* **1982**, *86*, 3819.

(35) Smith, C. A.; Molina, L. T.; Lamb, J. J.; Molina, M. J. *Int. J. Chem. Kinet.* **1984**, *16*, 41.

TABLE III: Equilibrium Constants for the Reactions



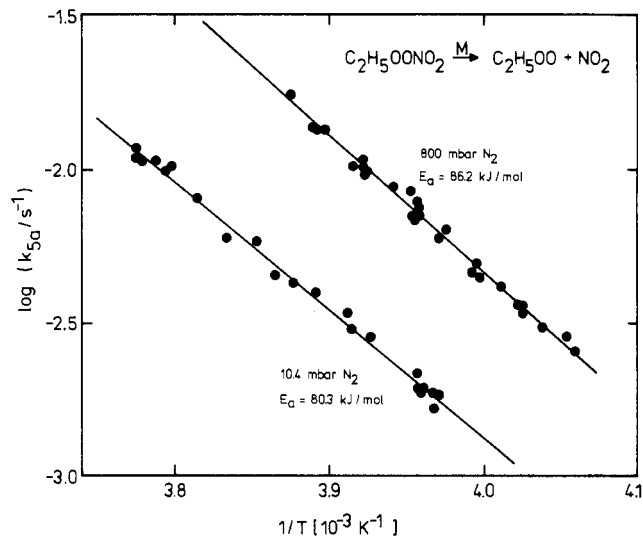
253 K, M = N <sub>2</sub>			
$p_{\text{tot}}$ , mbar	$k_{-1a}$ , 10 <sup>-12</sup> cm <sup>3</sup> molecule <sup>-1</sup> s <sup>-1</sup> (±2σ)	$k_{1a}$ <sup>a</sup> , 10 <sup>-3</sup> s <sup>-1</sup>	$K_c = k_{1a}/k_{-1a}$ , 10 <sup>8</sup> molecules cm <sup>-3</sup>
145	2.50 ± 0.34 <sup>b</sup>	1.68	6.72
333	3.85 ± 0.30 <sup>b</sup>	2.50	6.49
670	5.10 ± 0.50 <sup>b</sup>	3.35	6.57
692	5.8 ± 1.0 <sup>b</sup>	3.39	5.84
			av 6.41 ± 0.78 (2σ)
298 K, M = N <sub>2</sub>			
$p_{\text{tot}}$ , mbar	$k_{-1a}$ , 10 <sup>-12</sup> cm <sup>3</sup> molecule <sup>-1</sup> s <sup>-1</sup> (±2σ)	$k_{1a}$ <sup>c</sup> , 10 <sup>-3</sup> s <sup>-1</sup>	$K_c = k_{1a}/k_{-1a}$ , 10 <sup>11</sup> molecules cm <sup>-3</sup>
67	1.15 ± 0.20 <sup>d</sup>	0.419	3.64
101	1.36 ± 0.23 <sup>b</sup>	0.532	3.91
133	1.58 ± 0.30 <sup>d</sup>	0.618	3.91
209	1.90 ± 0.32 <sup>b</sup>	0.781	4.11
300	2.22 ± 0.62 <sup>d</sup>	0.937	4.22
344	2.60 ± 0.56 <sup>b</sup>	1.00	3.86
467	2.98 ± 0.46 <sup>d</sup>	1.16	3.89
469	2.82 ± 0.28 <sup>b</sup>	1.17	4.15
666	3.67 ± 0.42 <sup>d</sup>	1.37	3.73
692	3.36 ± 0.32 <sup>b</sup>	1.40	4.17
933	3.94 ± 0.34 <sup>d</sup>	1.59	4.04
962	4.12 ± 0.38 <sup>b</sup>	1.61	3.91
			av 3.96 ± 0.36 (2σ)

<sup>a</sup>This work, eq I. <sup>b</sup>Reference 7. <sup>c</sup>This work, extrapolation to 298 K by using eq I. <sup>d</sup>Reference 6.

in most measurements and performed two sets of experiments: (i) the temperature dependence at a constant pressure of 467 mbar between 256 and 268 K and (ii) the pressure dependence at a constant temperature between 67 and 960 mbar. In Figure 2, the present results and those of Bahta et al. are compared, demonstrating good agreement between both sets of data. From some experiments at 263.3 K and 980 mbar with M = CH<sub>4</sub> and with M = N<sub>2</sub>, Bahta et al. concluded that the collision efficiencies of N<sub>2</sub> and CH<sub>4</sub> are about the same. While the effect of these diluents on the first-order rate constant  $k_{1a}$  certainly may be similar at a total pressure of 980 mbar, which is fairly close to the high-pressure limit, a ratio of  $k_0(\text{M}=\text{CH}_4):k_0(\text{M}=\text{N}_2) \sim 3$  (see, e.g., ref 36) might be expected at the low-pressure limit. In fact, the slightly shallower falloff curve from the data of Bahta et al. (Figure 2) might indicate a corresponding shift of the falloff to lower pressures due to the higher collision efficiency of CH<sub>4</sub> as compared to N<sub>2</sub>.

The reverse reaction (-1a), the recombination of CH<sub>3</sub>OO radicals with NO<sub>2</sub>, has been extensively studied by two groups. Sander and Watson<sup>6</sup> studied reaction -1a at room temperature in the pressure range 67–933 mbar for different buffer gases (He, N<sub>2</sub>, SF<sub>6</sub>). From a least-squares fit of their rate constants  $k_{-1a}$  as a function of total pressure to eq I with  $N(F_c) = 1$ , they obtain  $F_c = 0.40 \pm 0.10$ , in agreement with the present work. Ravishankara et al.<sup>7</sup> determined  $k_{-1a}$  in a limited pressure range at three different temperatures (253, 298, and 353 K) for M = N<sub>2</sub>. Their measurements at 298 K are in very good agreement with the data of Sanders and Watson such that the temperature and pressure dependence of  $k_{-1a}$  can be considered to be well established. Using these recombination rate data and thermochemical arguments, Bahta et al.<sup>5</sup> deduced revised rate parameters for  $k_{1a}$  that are in good agreement with the present values.

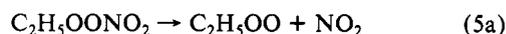
From the recombination rate data discussed above and the dissociation rate data from the present work, improved data on the equilibrium constant  $k_{1a}/k_{-1a}$  and the heat of formation of CH<sub>3</sub>OONO<sub>2</sub> can be deduced. For this purpose, the data points on  $k_{-1a}$  from Ravishankara et al.<sup>7</sup> for 253 K and M = N<sub>2</sub> at different total pressures are combined with the  $k_{1a}$  values obtained

Figure 3. Arrhenius plots of  $k_{5a}$  at different total pressures.

from the present work at 253 K for M = N<sub>2</sub>, using eq I for interpolation. The resulting equilibrium constants  $k_{1a}/k_{-1a}$  are included in Table III. As  $k_{1a}/k_{-1a}$  must be independent of pressure, the equilibrium constants at different pressures are averaged to give a final value of  $(6.5 \pm 0.9) \times 10^8$  molecule cm<sup>-3</sup> (±2σ) at 253 K. Similarly, the  $k_{1a}(T)$  data from the present work are extrapolated to the conditions of Ravishankara et al.<sup>7</sup> and of Sander and Watson<sup>6</sup> at 298 K, using eq I. The equilibrium constants thus obtained are included in Table III and give an average value of  $(3.9 \pm 0.4) \times 10^{11}$  molecule cm<sup>-3</sup> (±2σ).

From the equilibrium constants at 253 and 298 K, a heat of reaction of  $\Delta H_r^\circ_{273} = 91.8 \pm 3.4$  kJ mol<sup>-1</sup> is deduced. The temperature dependence of  $K_c = k_{1a}/k_{-1a}$  is represented by the expression  $K_c = 1.94 \times 10^{27} \exp(-10766 \text{ K}/T)$  molecule cm<sup>-3</sup>. Conversion of  $\Delta H_r^\circ$  to 298 K using the vibrational frequencies of CH<sub>3</sub>OONO<sub>2</sub> from Table II and of CH<sub>3</sub>OO and NO<sub>2</sub> from Patrick and Golden<sup>27</sup> gives  $\Delta H_r^\circ_{298} = 92.2 \pm 3.4$  kJ mol<sup>-1</sup> for reaction 1a. With the heats of formation of CH<sub>3</sub>OO and NO<sub>2</sub> from DeMore et al.,<sup>30</sup>  $\Delta H_f^\circ_{298}(\text{CH}_3\text{OONO}_2) = -43 \pm 11$  kJ mol<sup>-1</sup> is obtained, where the error limits mainly reflect the uncertainty of  $\Delta H_f^\circ_{298}(\text{CH}_3\text{OO})$ . This result is in good agreement with the value  $\Delta H_f^\circ_{298}(\text{CH}_3\text{OONO}_2) = -44.4$  kJ/mol<sup>30,37</sup> estimated by using thermochemical arguments.

**Ethyl Peroxynitrate.** At temperatures below 0 °C, ethyl peroxynitrate was stable in the reaction chamber for large [NO<sub>2</sub>]/[NO] ratios but unstable for small [NO<sub>2</sub>]/[NO] ratios. This demonstrates that C<sub>2</sub>H<sub>5</sub>OONO<sub>2</sub> decomposes via OO-N bond fission like CH<sub>3</sub>OONO<sub>2</sub>. Different from the experiments on CH<sub>3</sub>OONO<sub>2</sub>, the temperature dependence of  $k_{5a}$



was measured at two very different total pressures (800 mbar and 10.4 mbar, M = N<sub>2</sub>), and the pressure dependence of  $k_{5a}$  was determined in this pressure range at a single temperature (253 K). The first-order gas-phase decomposition rate constants of C<sub>2</sub>H<sub>5</sub>OONO<sub>2</sub>,  $k_{5a}$ , as a function of temperature and pressure are summarized in Table IV. The temperature dependence of  $k_{5a}$  is presented in Figure 3. As the experiments at a total pressure of 800 mbar are close to the high-pressure limit, the experimental activation energy at this pressure is taken as a first-order estimate of  $E_{a\infty}$ ; i.e.,  $E_{a\infty} = 86.2$  kJ mol<sup>-1</sup>. The low-pressure activation energy  $E_{a0}$  was estimated according to the equation  $E_{a0} \approx E_{a\infty} - (S_{\text{eff}} \pm 0.5)RT$  from Luther and Troe,<sup>20</sup> using the vibrational frequencies 3000 (5×), 1719, 1700, 1400 (5×), 1300, 1055 (2×), 1000 (3×), 988, 880, 821, 791, 716, 488, 370, 338, 120 (2×), and 45 (2×); see Table II for comparison. The falloff parameter  $F_c$  was estimated from these frequencies according to the methods

(36) Baulch, D. L.; Cox, R. A.; Hampson, R. F., Jr.; Kerr, J. A.; Troe, J.; Watson, R. T. *J. Phys. Chem. Ref. Data* 1980, 9, 295.

(37) Baldwin, A. C. Thermochemistry of Peroxides. In *Chemistry of Functional Groups*; Patai, S., Ed.; Wiley: New York, 1982.

**TABLE IV: Summary of First-Order Rate Constants for the Thermal Decomposition ( $k_{5a}$ ) and Wall Loss ( $k_{5b}$ ) of  $C_2H_5OONO_2$** 

run no.	$T$ , K	$p_{tot}$ , mbar ( $M = N_2$ )	$k_{5a}$ , $10^{-4} s^{-1}$	$k_{5b}$ , $10^{-4} s^{-1}$	$k_{5a,av}(253 K)$ , $10^{-4} s^{-1} (2\sigma)$
1	245.45	800	18.9	0.6	
2	246.35	800	25.4	0.4	
3	246.7	800	28.3	0.4	
4	247.65	800	30.3	1.0	
5	248.5	800	35.9	0.5	
6	248.5	800	33.6	1.2	
7	248.65	800	35.7	1.4	
8	249.35	802	40.9	0.6	
9	250.15	800	55.4	0.7	
10	250.3	800	48.9	0.7	
11	250.55	800	43.8	0.7	
12	251.55	800	63.4	0.4	
13	251.75	802	58.8	0.6	
14	251.85	800	59.6	0.6	
15	252.65	799	70.5	0.5	
16	252.65	801	74.9	0.0	
17	252.75	800	78.9	0.4	$76.6 \pm 12.3$
18	252.9	800	68.1	0.6	
19	253.0	800	70.5	0.7	
20	253.05	800	84.8	0.7	
21	253.75	800	87.2	0.0	
22	254.85	800	99.2	0.7	
23	254.95	800	96.1	0.7	
24	255.0	800	108	0.4	
25	255.05	800	99.7	0.5	
26	255.45	801	102	0.0	
27	256.6	799	135	0.1	
28	257.0	802	137	0.0	
29	257.15	801	139	0.6	
30	258.1	802	176	0.0	
31	252.05	302	59.2	0.9	
32	252.6	301	58.9	0.7	$64.2 \pm 8.4$
33	253.05	304	61.4	0.0	
34	252.45	101	42.3	0.5	
35	252.7	100	45.8	0.8	
36	252.8	104	42.5	0.6	$46.7 \pm 3.4$
37	252.8	100	46.3	1.0	
38	253.05	101	47.7	0.4	
39	252.65	30.0	29.8	1.0	
40	252.75	30.1	31.1	0.7	$32.9 \pm 3.3$
41	253.4	30.1	37.0	0.7	
42	251.85	10.2	18.5	1.0	
43	252.05	10.2	18.6	0.7	
44	252.05	10.1	16.6	1.0	
45	252.5	10.3	19.3	1.3	
46	252.55	10.1	19.0	0.6	$20.8 \pm 2.2$
47	252.55	10.2	18.7	0.4	
48	252.75	10.3	19.4	0.8	
49	252.75	10.3	21.5	0.6	
50	254.7	10.5	28.7	0.9	
51	255.45	10.6	30.1	0.2	
52	255.65	11.1	34.2	0.5	
53	256.95	10.5	39.9	0.0	
54	257.95	10.4	42.3	0.5	
55	258.75	10.4	45.0	0.5	
56	259.55	10.5	51.2	0.7	
57	260.85	10.5	59.9	0.8	
58	262.15	10.6	81.2	1.8	
59	263.3	10.6	103	0.0	
60	263.6	10.5	98.3	0.0	
61	264.05	10.1	107	0.7	
62	264.95	10.6	110	0.0	
63	264.95	10.6	119	1.6	

of Troe et al.<sup>20-22</sup> to be  $\sim 0.29$ , allowing for weak collision effects (with the estimate  $k_0/k_0^{sc} \sim 0.2$  for  $M = N_2$ ). Considering the uncertainties of this estimate, a value of  $F_c = 0.3$  was adopted for the analysis of the present rate data. Absolute values for  $k_0$  and  $k_\infty$  were obtained by fitting a reduced falloff curve for  $F_c = 0.3$  to the experimental results at 253 K and different total pressures (see Figure 4). From these absolute values for  $k_0$  and

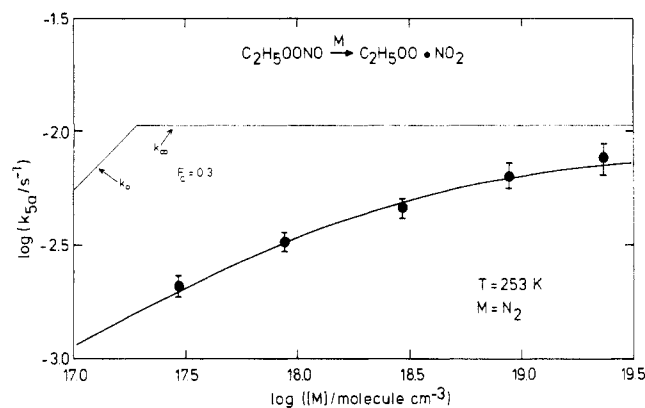


**Figure 4.** Pressure dependence of  $k_{5a}$  at 253 K for  $M = N_2$ .  $\odot$ , average of at least four individual rate constants; straight lines,  $k_0 = k_{2nd\ order}[N_2]$  and  $k_\infty$ .

**TABLE V: First-Order Decomposition Rate Constants  $k_{6a}$ ,  $k_{7a}$ , and  $k_{8a}$  for  $C_4H_9OONO_2$ ,  $C_6H_{13}OONO_2$ , and  $C_8H_{17}OONO_2$  (Isomeric Mixtures) at 253 K and 800 mbar**

run no.	R	$T$ , K	$p_{tot}$ , mbar ( $M = N_2$ )	$k_a$ , $10^{-4} s^{-1}$	$k_{a,av}(253 K)$ , $10^{-4} s^{-1} (2\sigma)$
1	$C_4H_9$	252.5	800	124	$133 \pm 20$
2	$C_4H_9$	252.65	800	124	
3	$C_6H_{13}$	252.5	800	106	
4	$C_6H_{13}$	252.7	800	131	$120 \pm 30$
5	$C_6H_{13}$	254.0	800	127	
6	$C_8H_{17}$	253.9	800	69	$76 \pm 25$
7	$C_8H_{17}$	252.65	800	87	

$k_\infty$  at 253 K, from the above first-order approximations for  $E_{a0}$  and  $E_{a\infty}$ , and with  $F_c = 0.3$ , activation energies can be calculated for total pressures of 800 mbar and 10.2 mbar, using eq I. The derived activation energies are too low by  $1.4 kJ mol^{-1}$  and too high by  $0.2 kJ mol^{-1}$  at 800 and 10.2 mbar, respectively, as compared to the experimental values from Figure 3. For this reason, the finally selected values for  $E_{a\infty}$  and  $E_{a0}$  are higher by  $0.6 kJ mol^{-1}$ , giving rise to activation energies at 800 and 10.2 mbar which deviate from the experimental values by  $+0.8$  and  $-0.8 kJ mol^{-1}$ . This difference is well within the experimental error limits. Thus all of the present kinetic data on  $k_{5a}$  are well reproduced by eq I and the following parameters:

$$F_c = 0.3$$

$$k_0/[N_2] = 4.8 \times 10^{-4} \exp(-77.2 kJ mol^{-1}/RT) cm^3 molecule^{-1} s^{-1}$$

$$k_\infty = 8.8 \times 10^{15} \exp(-86.8 kJ mol^{-1}/RT) s^{-1}$$

There are no results on  $k_{5a}$  in the literature to compare with. The reverse reaction  $k_{-5a}$  has been measured at room temperature by Adachi and Basco.<sup>13</sup> No pressure dependence was observed by these authors for  $k_{-5a}$  at total pressures between 60 and 900 mbar, while  $k_{5a}$  changes by a factor of 2 in the present experiments within the same pressure range. There are indications, however, that the UV detection of ethylperoxy radicals in the work of Adachi and Basco might have suffered from interference with the absorption by reaction products (see, e.g., discussions in ref 6 and 38).

**Higher Alkyl Peroxynitrates.** For *n*-alkanes with more than two carbon atoms, isomeric mixtures of alkyl peroxynitrates are formed in the photolysis of  $RH/Cl_2/NO_2/O_2$  mixtures. The isomers could not be differentiated from one another using IR absorption in the present experiments. However, it is expected that the isomeric peroxynitrates decompose with similar rates. For this reason, some experiments were performed on the thermal decomposition of isomeric mixtures of butyl, hexyl, and octyl peroxynitrate at 253 K and 800 mbar total pressure in nitrogen.

(38) Plumb, I. C.; Ryan, K. R.; Steven, J. R.; Mulcahy, M. F. R. *Int. J. Chem. Kinet.* **1982**, *14*, 183.

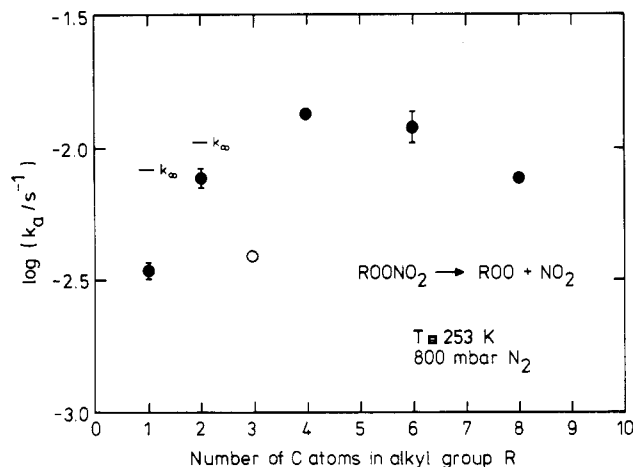
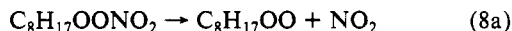


**Figure 5.** First-order decay rate constants  $k_a$  for the reactions  $\text{ROONO}_2 \rightarrow \text{ROO} + \text{NO}_2$  at 253 K in 800 mbar of  $\text{N}_2$  as a function of increasing complexity of alkyl group R.  $\bullet$ , present work, average of at least three individual rate constants with  $2\sigma$  errors;  $\bullet$ , present work, average of two individual rate constants;  $\circ$ , Edney et al.;<sup>14</sup> values of  $k_a$  for R =  $\text{CH}_3$  and  $\text{C}_2\text{H}_5$  from the present work.

The results are summarized in Table V and are presented in Figure 5 as a function of the complexity of R, including the rate constants for  $\text{CH}_3\text{OONO}_2$  and  $\text{C}_2\text{H}_5\text{OONO}_2$  at the same reaction conditions from Tables I and IV. It is interesting to note that, with increasing number of C atoms in the alkyl group R, the rate constants  $k_a$  increase up to R = *n*-butyl but then decrease again. This latter behavior may be caused by both a slightly increasing OO–N bond energy and/or the increasing distance from the high-pressure limit. It is assumed that, for atmospheric applications, the decomposition rate constants can be considered to be pressure independent. Probably, the activation energy of  $k_{5a}$  at 800 mbar is a good first-order approximation for the activation energies of  $k_{6a}$ ,  $k_{7a}$ , and  $k_{8a}$ .



Thus the following Arrhenius expressions are obtained from the rate constants in Table V:

$$k_{6a} \sim 8.3 \times 10^{15} \exp(-86.2 \text{ kJ mol}^{-1}/RT) \text{ s}^{-1}$$

$$k_{7a} \sim 7.5 \times 10^{15} \exp(-86.2 \text{ kJ mol}^{-1}/RT) \text{ s}^{-1}$$

$$k_{8a} \sim 4.8 \times 10^{15} \exp(-86.2 \text{ kJ mol}^{-1}/RT) \text{ s}^{-1}$$

By interpolating between the rate constants  $k_{5a}$  and  $k_{6a}$  in Figure 5,  $k_{9a} \sim 1.0 \times 10^{-2} \text{ s}^{-1}$  is obtained for R =  $\text{C}_3\text{H}_7$ , at 253 K and 800 mbar.



This may be compared with the value  $k_{9a} \sim 3.9 \times 10^{-3}$  which can be derived from an Arrhenius expression for  $k_{9a}$  presented by Edney et al.<sup>14</sup> Their experiments were performed close to room temperature at large  $[\text{NO}_2]/[\text{NO}]$  ratios, that is, under reaction conditions where the effective first-order decay rate of the per-

oxynitrate is much slower than the unimolecular decay. Thus their results on  $k_{9a}$  largely depend on the correct ratio for the rate constants of the reactions of  $\text{C}_3\text{H}_7\text{OO}$  radicals with  $\text{NO}$  and  $\text{NO}_2$ . If the more recent value of  $\sim 1$  for this ratio (for R = ethyl, propyl, ...<sup>23,38,39</sup>) is used instead of the value 2.4 which Edney et al. applied, excellent agreement is achieved between the experimental value for  $k_{9a}$  of Edney et al. and the above estimate based on Figure 5.

**Atmospheric Relevance.** From eq I and the values for  $k_0$ ,  $k_\infty$ , and  $F_2$  from the present work, rate constants  $k_a$  can be estimated for relevant atmospheric conditions. For the pressures and temperatures of the U.S. standard atmosphere,<sup>40</sup> the thermal lifetimes of  $\text{CH}_3\text{OONO}_2$  and  $\text{C}_2\text{H}_5\text{OONO}_2$  increase from 2 and 1 s at ground level (288 K, 1 atm) to a maximum of  $1 \times 10^6$  and  $2 \times 10^5$  s, respectively, in the tropopause and then decrease again with thermal lifetimes of  $5 \times 10^5$  and  $3 \times 10^5$  s at a height of 25 km. It has been already pointed out by Bahta et al.<sup>5</sup> that  $\text{CH}_3\text{OONO}_2$  may represent an important reservoir of  $\text{NO}_x$  in the lower stratosphere. The same is true, to a lesser extent, for  $\text{C}_2\text{H}_5\text{OONO}_2$  and higher alkyl peroxy nitrates. In addition, a large fraction of odd nitrogen and  $\text{CH}_3\text{OO}$  and  $\text{C}_2\text{H}_5\text{OO}$  radicals may be tied up in  $\text{CH}_3\text{OONO}_2$  and  $\text{C}_2\text{H}_5\text{OONO}_2$  in the upper troposphere where the alkyl peroxy nitrates can take part in the long-range transport of  $\text{NO}_x$  that has been observed for acetyl peroxy nitrates (PAN).<sup>41</sup> The role of alkyl peroxy nitrates in the troposphere has been estimated by Brewer et al.<sup>42</sup> in model calculations, including  $\text{HOONO}_2$ , PAN,  $\text{CH}_3\text{OONO}_2$ , and  $\text{ROONO}_2$ . They conclude that the integrated column content from the surface to the tropopause is an order of magnitude lower for  $\text{CH}_3\text{OONO}_2$  as compared to  $\text{HOONO}_2$  and PAN, and even much lower for  $\text{ROONO}_2$  (R = alkyl larger than methyl). On the other hand, the relative importance of  $\text{CH}_3\text{OONO}_2$  and  $\text{ROONO}_2$  could be much higher in the upper troposphere with its lower temperature. For a more precise assessment of the role of  $\text{CH}_3\text{OONO}_2$ ,  $\text{C}_2\text{H}_5\text{OONO}_2$ , and higher alkyl peroxy nitrates in the atmosphere to be made, the photolysis rates and products must be known more accurately, in particular for wavelengths close to 300 nm.

## Conclusions

The thermal decomposition of  $\text{CH}_3\text{OONO}_2$  (reaction 1a) and  $\text{C}_2\text{H}_5\text{OONO}_2$  (reaction 5a) has been investigated for M =  $\text{N}_2$  in a wide temperature and pressure range, and the limiting low- and high-pressure rate constants for M =  $\text{N}_2$  have been determined. Combining the present and previous<sup>5</sup> work on  $k_{1a}$  with literature data on  $k_{-1a}$ , the system  $\text{CH}_3\text{OONO}_2 \rightleftharpoons \text{CH}_3\text{OO} + \text{NO}_2$  seems to be well characterized, suggesting  $\text{CH}_3\text{OONO}_2$  to be an important reservoir for both  $\text{NO}_x$  and  $\text{CH}_3\text{OO}$  radicals in the upper troposphere and the lower stratosphere. Higher alkyl peroxy nitrates might add considerably to these  $\text{NO}_x$  and ROO reservoirs.

**Acknowledgment.** Financial support of this work by the "Deutsche Forschungsgemeinschaft (DFG)" and by the "Bundesminister für Forschung und Technologie (BMFT)" is gratefully acknowledged.

**Registry No.**  $\text{CH}_3(\text{O})_2\text{NO}_2$ , 42829-59-4;  $\text{C}_2\text{H}_5(\text{O})_2\text{NO}_2$ , 64160-40-3;  $\text{C}_4\text{H}_9(\text{O})_2\text{NO}_2$ , 120712-03-0;  $\text{C}_6\text{H}_{13}(\text{O})_2\text{NO}_2$ , 120712-04-1;  $\text{C}_8\text{H}_{17}(\text{O})_2\text{NO}_2$ , 120712-05-2.

(40) U.S. Standard Atmosphere 1976. Cited in Brasseur, G.; Solomon, S.; *Aeronomy of the Middle Atmosphere*; Reidel: Dordrecht, 1984.

(41) Nielsen, T.; Samuelsson, U.; Grennfelt, P.; Thomsen, E. L. *Nature* **1981**, 293, 553.

(42) Brewer, D. A.; Augustsson, T. R.; Levine, J. S. *J. Geophys. Res.* **1983**, 88, 6683.

(39) Elfers, G.; Zabel, F. Presented at the COST 611 Working Party 2 Meeting, 20–22 September 1988, Norwich, U.K..